Development 139, 95-105 (2012) doi:10.1242/dev.069294

Basolateral rather than apical primary cilia on neuroepithelial cells committed to delamination

Michaela Wilsch-Bräuninger, Jula Peters, Judith T. M. L. Paridaen and Wieland B. Huttner*

SUMMARY

Delamination of neural progenitors from the apical adherens junction belt of the neuroepithelium is a hallmark of cerebral cortex development and evolution. Specific cell biological processes preceding this delamination are largely unknown. Here, we identify a novel, pre-delamination state of neuroepithelial cells in mouse embryonic neocortex. Specifically, in a subpopulation of neuroepithelial cells that, like all others, exhibit apical-basal polarity and apical adherens junctions, the re-establishing of the primary cilium after mitosis occurs at the basolateral rather than the apical plasma membrane. Neuroepithelial cells carrying basolateral primary cilia appear at the onset of cortical neurogenesis, increase in abundance with its progression, selectively express the basal (intermediate) progenitor marker Tbr2, and eventually delaminate from the apical adherens junction belt to become basal progenitors, translocating their nucleus from the ventricular to the subventricular zone. Overexpression of insulinoma-associated 1, a transcription factor known to promote the generation of basal progenitors, increases the proportion of basolateral cilia. Basolateral cilia in cells delaminating from the apical adherens junction belt are preferentially found near spot-like adherens junctions, suggesting that the latter provide positional cues to basolateral ciliogenesis. We conclude that re-establishing a basolateral primary cilium constitutes the first known cell biological feature preceding neural progenitor delamination.

KEY WORDS: Basal progenitor, Cell polarity, Neuroepithelium, Neurogenesis, Primary cilium, Mouse

INTRODUCTION

Delamination of epithelial cells is a fundamental process in tissue morphogenesis during development. A striking example of delamination is the development of the mammalian cerebral cortex, which originates from the dorsolateral telencephalic neuroepithelium. The primary stem and progenitor cells of this tissue, the neuroepithelial cells (NECs), exhibit apical-basal polarity, a central parameter in the delamination process (Götz and Huttner, 2005). Notably, these cells remain in contact with the basal lamina throughout the cell-cycle via their basal plasma membrane, are anchored to each other by an adherens junction (AJ) belt at the apical-most end of their lateral plasma membrane and possess an apical plasma membrane that constitutes the ventricular surface (Farkas and Huttner, 2008). As in other epithelial cells with apical-basal polarity (Weisz and Rodriguez-Boulan, 2009), a primary cilium (from here onwards referred to simply as 'cilium') emanates from the apical plasma membrane of NECs (Cohen and Meininger, 1987; Dubreuil et al., 2007; Farkas and Huttner, 2008; Hinds and Ruffett, 1971; Sotelo and Trujillo-Cenoz, 1958).

In the course of centrosome duplication during the cell cycle, the cilium's basal-body and its associated second centriole each become the template centriole of the two centrosomes that during M-phase form the poles of the mitotic spindle (Bettencourt-Dias and Glover, 2007; Nigg and Raff, 2009). Consequently, given that the cilium persists during the cell cycle until the onset of M-phase, its apical location in NECs is considered to be the main reason why their nuclei undergo mitosis at the ventricular surface (Taverna and Huttner, 2010). This in turn is why NECs and the highly related radial glial cells into which they transform with the onset of neurogenesis (Kriegstein and Alvarez-Buylla, 2009) have been referred to collectively as apical progenitors (APs) (Farkas and Huttner, 2008; Taverna and Huttner, 2010). APs span the entire cortical wall, with their nuclei undergoing interkinetic nuclear migration (Taverna and Huttner, 2010) in the ventricular zone (VZ).

During cerebral cortex development, AP divisions are symmetric initially, with each division generating two daughter APs, both of which exhibit apical-basal polarity and re-establish a cilium at their apical plasma membrane after mitosis, utilizing the centrosome inherited from the mother AP (Farkas and Huttner, 2008; Kriegstein and Alvarez-Buylla, 2009). With the onset of cortical neurogenesis, an increasing proportion of APs switch to asymmetric divisions. These result in AP self-renewal and the generation of either a neuron destined for the preplate/cortical plate or, more frequently, a distinct type of progenitor, referred to as basal progenitor (BP) or intermediate progenitor cell, destined for the subventricular zone (SVZ) (Götz and Huttner, 2005; Kriegstein and Alvarez-Buylla, 2009). At birth, depending on the orientation of the cleavage plane relative to the apical plasma membrane and AJ belt, these neurons and BPs can be delaminated already, i.e. are no longer integrated into this belt and lack apical plasma membrane (Fietz and Huttner, 2010; Konno et al., 2008). Alternatively, the newborn neurons and BPs can initially be integrated into the AJ belt and possess apical plasma membrane, and subsequently delaminate from this belt and become devoid of apical plasma membrane (Konno et al., 2008).

Mature CNS neurons are known to carry a cilium on their perikaryal surface (Lee and Gleeson, 2010; Louvi and Grove, 2011). It is unknown, however, at which stage in the neuronal differentiation process the centrosome inherited from the neuronal progenitor cell is utilized for ciliogenesis (Han and Alvarez-Buylla,

Max-Planck-Institute of Molecular Cell Biology and Genetics, Pfotenhauer Strasse 108, D-01307 Dresden, Germany.

*Author for correspondence (huttner@mpi-cbg.de)

Accepted 27 October 2011

2010). Similarly, assuming that BPs (like most cell types) carry a cilium, it is unknown when during the BP life cycle the centrosome inherited from the AP is utilized for ciliogenesis. In this context, an important question arising is whether ciliogenesis is in any way related to BP/neuron delamination.

The process of ciliogenesis includes two major steps, (1) membrane association of the centrosome's older centriole, which becomes the cilium's basal body, and (2) growth of the microtubule-based axonemes in concert with the evagination of the ciliary membrane (Marshall, 2008; Pazour and Bloodgood, 2008; Pedersen et al., 2008; Rohatgi and Snell, 2010; Rosenbaum and Witman, 2002; Santos and Reiter, 2008; Satir and Christensen, 2007; Sorokin, 1968). These steps can occur either at the plasma membrane or at intracellular membranes, such as Golgi-derived or endosomal membrane vesicles that subsequently fuse with the plasma membrane.

Given that the cilium has been shown to be a key organelle in cell signalling (Berbari et al., 2009; Goetz and Anderson, 2010; Lancaster and Gleeson, 2009), the cilium protruding from the apical plasma membrane of APs is in a strategic location to detect signals in the ventricular fluid (Han and Alvarez-Buylla, 2010). This option no longer exists for neurons and BPs after they have delaminated from the AJ belt and become devoid of apical plasma membrane. Key questions arising from these considerations are when those newborn neurons and BPs that are initially integrated into the AJ belt and possess apical plasma membrane re-establish a cilium, and on which membrane. Here, we show that such newborn BPs re-establish the cilium on their basolateral, rather than apical, plasma membrane. Re-establishing a basolateral (bl)-cilium therefore emerges as the first known cell biological feature that precedes BP delamination, a key aspect of cerebral cortex evolution.

MATERIALS AND METHODS

Mice

Unless otherwise indicated, C57BL/6 mice were used. The transgenic mouse line expressing *Tbr2*-GFP was the Tg(Eomes::GFP) BAC transgenic strain described previously (Gong et al., 2003; Kwon and Hadjantonakis, 2007). All animal studies were conducted in accordance with German animal welfare legislation.

Conventional transmission electron microscopy (EM)

Fixed embryos at embryonic day (E) 9.5-17.5 were embedded in 4% low-melting agarose (ScienceServices) in 0.1 M phosphate buffer pH 7.4, followed by the preparation of transverse 200-μm-thick vibratome sections (VT1200S, Leica). Sections were fixed in 1% glutaraldehyde in 0.1 M phosphate buffer for at least 1 hour, post-fixed in 1% osmium tetroxide, contrasted with 1% uranyl acetate, dehydrated and flat-embedded in Epon replacement (Carl Roth).

Ultrathin (70 nm) plastic sections of dorsal telencephalon (dTel) and hindbrain were cut on a microtome (Leica, UCT) and post-stained with uranyl acetate and lead citrate according to standard protocols. Images were taken on a Morgagni EM at 80 kV (FEI) with a Morada or Veleta camera (Olympus) and ITEM software (Olympus).

Post-embedding immunolabelling for light and electron microscopy

Vibratome sections of E12.5-13.5 mouse embryos prepared as above were embedded in 12% gelatin in 0.1 M phosphate buffer. Gelatin-embedded tissue pieces containing dTel were infiltrated with 2.3 M sucrose for Tokuyasu cryosectioning (140 nm for immunofluorescence, 70 nm for EM). For both immunofluorescence and immuno-electron microscopy (immuno-EM), sections were immunolabelled as previously described for ultrathin cryosections (Dubreuil et al., 2007) using mouse mAbs against actin (Linaris, 1:10), pan-cadherin (Sigma, 1:50), β-catenin (BD, 1:50), polyglutamylated tubulin (Enzo, 1:100), rat mAb against integrin-α6 (Chemicon, 1:5); rabbit antibodies against Arl13b (ProteinTech, 1:100), β-catenin (Sigma, 1:200), Cep164 (ProSci, 1:20), GFP (Abcam, 1:150), Odf2 (Abcam, 1:10), Tbr2 (Abcam, 1:50) and γ-tubulin (Sigma, 1:200); and goat antibody against GFP (MPI-CBG, 1:150), followed by Cy3- or Cy2-conjugated goat anti-mouse, goat anti-rabbit, donkey anti-rabbit or donkey anti-goat secondary antibodies for immunofluorescence (Dianova, 1:400) and goat anti-mouse IgG/5-nm or 10-nm-gold (Dianova, 1:30) or proteinA/10-nm-gold (University Utrecht) for EM. The lipid GM1 was detected using Alexa488-coupled cholera toxin-subunit B (Sigma, 1:50) followed by a rabbit anti-Alexa488 antibody (Invitrogen, 1:500) and proteinA/10-nm-gold. Immunofluorescence sections were embedded in Mowiol 4-88 and viewed using a conventional fluorescence microscope [Olympus BX61 or Zeiss Axiovert 200M, both with Diagnostic Instrument cameras with IPLab (BD) or MetaMorph (Molecular Devices) software]. EM micrographs were taken as described above.

Pre-embedding immuno-EM

E11.5-13.5 *Tbr2*-GFP embryos were dissected and fixed in 4% paraformaldehyde in 0.1 M phosphate buffer, and 200-μm-thick vibratome sections were cut, permeabilized with 0.1% Triton X-100 and blocked with 0.5% bovine serum albumin (Sigma), 0.2% gelatin in PBS. Sections were incubated with rabbit anti-GFP antibodies (Abcam ab290, 1:1500) followed by goat anti-rabbit-IgG antibody coupled to ultrasmall gold (Aurion, The Netherlands, 1:100). Sections were fixed in 1% glutaraldehyde, processed for silver enhancement (R-Gent SE-EM, Aurion) and post-fixed in 1% osmium tetroxide followed by embedding as described above for conventional transmission EM.

Pre-embedding labelling for prominin-1 was performed as described (Dubreuil et al., 2007), either without modification or by replacing the protein A/10-nm-gold by ultrasmall gold and silver enhancement as described above. As the latter labelling was, in principle, the same as that used to detect *Tbr2*-GFP, which resulted in labelling throughout the cytoplasm, the lack of prominin-1 labelling on the bl-plasma membrane was not due to lack of penetration of the antibodies or detection reagents used.

Quantification of apical versus bl-cilia

Apical versus bl-cilia were quantified on ultrathin plastic sections that were oriented largely parallel to the apical-basal axis of ventricular cells. To avoid scoring the same cilium in different sections, only every ≥4th consecutive section was analysed. Quantification was confined to the apical-most ≈5 μm of the VZ. Only cells that, in the section analysed, either showed apical plasma membrane or at least formed apical AJs with neighbouring cells were used for quantification. We considered only cilia that showed a basal body in the section analysed and that protruded from the membrane for at least 400 nm, using the width of the basal body (≈200 nm) as the measuring unit, provided that they did not show the 'chubby' appearance of nascent cilia (Sorokin, 1962; Sotelo and Trujillo-Cenoz, 1958). Cilia were scored as apical if they, in the section analysed, either protruded into the ventricular lumen or were present in a membrane profile that was within 500 nm or less of the ventricular surface, which, hence, could be assumed to be obliquely sectioned apical plasma membrane. Cilia were scored as bl-type if they either protruded into the intercellular space or were present in a membrane profile that was basal to the AJ belt, which, hence, could be assumed to be obliquely sectioned bl-plasma membrane. Statistical significance was determined using an unpaired *t*-test (with Welch's correction) in R (http://www.R-project.org/).

Insm1 overexpression

In utero electroporation of dTel of E12.5 embryos with pCAGGS-GFP (0.3 μg/μl) in combination with, or without, pCMV-SPORT6-*Insm1* (1.5 μg/μl) was performed as described (Farkas et al., 2008).

The effect of *Insm1* overexpression on the occurrence of bl-cilia was determined for GFP-positive cells 12 and 18 hours after electroporation. Using ultrathin, post-embedding GFP-immunogold-labelled frozen sections, the apical-most region of the neuroepithelium was analysed. As some of the sections analysed were consecutive and, therefore, the same single cilium could be scored in multiple sections, the cilia numbers of

every third section were pooled and summed up, yielding three values, as follows: section numbers 1+4+7, etc.; section numbers 2+5+8, etc.; section numbers 3+6+9, etc. Section and embryo numbers were: control 12 hours: 20 sections from one embryo; *Insm1* 12 hours: 45 sections from two embryos; control 18 hours: 31 sections from three embryos; *Insm1* 18 hours: 55 sections from two embryos. Statistical significance was determined using an unpaired, one-tailed *t*-test. Sections of the same series were subjected to Tbr2 and GFP double immunofluorescence; each count was the sum of two to three sections.

Colocalization of bl-cilia and spot-like AJs

The numbers of bl-cilia and spot-like AJs basal to the apical AJ belt (i.e. excluding the apical-most ≈2 μm region of the VZ) were counted by scanning β-catenin- and polyglutamylated tubulin-immunogold-labelled ultrathin frozen sections that contained at least one bl-cilium under the electron microscope. A bl-cilium and a spot-like AJ were scored as colocalized if the gap between these two structures (in the case of the bl-cilium, typically the basal body) was ≤500 nm; when including the size of the basal body and that of a spot-like AJ, such a bl-cilium/spot-like AJ assembly was found to be ≤1.2 μm.

For calculating the probability of colocalization of bl-cilia and spot-like AJs, the radial thickness of the VZ was measured on micrographs of the ultrathin frozen sections analysed. The probability of colocalization was calculated assuming a binominal distribution according to $P=1-(1-\text{size of assembly/length of lateral membrane})^{\text{number of junctions per lateral membrane}}$.

Terminology

A 'ventricular cell' (VC) is defined as a cell that contains apical plasma membrane and is integrated in the AJ belt. This term thus comprises neuroepithelial/radial glial cells carrying apical cilia and cells with ventricular contact that carry bl-cilia.

'Basolateral-type cilia' is the collective term for bl-cilia of VCs and cilia of delaminated cells; that is, cells that show neither apical plasma membrane nor contact with the apical AJ belt. The latter cilia comprise both cilia protruding into the intercellular space and cilia surrounded by membrane in the section analysed.

RESULTS

Primary cilia of neuroepithelial cells occur not only on the apical but also on the basolateral plasma membrane

EM of the VZ of mouse embryonic day (E) 12.5-13.5 dTel revealed numerous primary cilia protruding from the apical plasma membrane of neuroepithelial cells (NECs) into the ventricular lumen (Fig. 1A), as described previously (Cohen and Meininger, 1987; Dubreuil et al., 2007; Hinds and Ruffett, 1971; Sotelo and Trujillo-Cenoz, 1958). Remarkably, however, some cilia also emerged from the basolateral (bl) plasma membrane of NECs (Fig. 1B-F). Importantly, these cells appeared to be unaltered with regard to other features of apical cell polarity, such as, exhibiting an apical plasma membrane and apical AJs (Fig. 1C,E). In light of the findings described below that such cells with bl-cilia lose apical polarity and, hence, neuroepithelial character, we shall from here onwards refer to these cells as ventricular (rather than neuroepithelial) cells (see note on terminology in Materials and methods).

EM analysis also provided evidence that the bl-plasma membrane was the final destination of bl-cilia. The two centrioles at the base of some bl-cilia had undergone duplication (Fig. 1E,F), indicating that the respective ventricular cell (VC) had progressed beyond the G1 phase of its cell cycle (Bettencourt-Dias and Glover, 2007; Nigg and Raff, 2009; Santos and Reiter, 2008; Seeley and Nachury, 2010). Ciliogenesis in cycling cells is known to take place early in G1. Hence, bl-cilia did not constitute an intermediate in apical ciliogenesis, being in transit to the ventricular surface, but were mature cilia.

Bl-cilia either, in the minority of cases, fully protruded from the bl-membrane into the intercellular space, occasionally being largely surrounded by bl-membrane of a neighbouring NEC (Fig. 1C,D), or, in the majority of cases, were embedded in a ciliary pocket with a small opening to the intercellular space (Fig. 1E; supplementary material Fig. S1A-F). The majority of bl-cilia pointed basally. The fine structure of bl-cilia resembled that of canonical cilia (including apical cilia of NECs), with a 9+0 microtubule doublet axoneme (Fig. 1G,H) extending from a basal body with nearby centriolar satellites (Fig. 1E). In addition, transitional fibres (also called alar sheets or distal appendages) and subdistal appendages, two structures that are thought to tether the cilium to the plasma membrane, and a necklace structure of the plasma membrane at the ciliary base were observed (Fig. 1D,F) (Cohen and Meininger, 1987; Dawe et al., 2007; Satir and Christensen, 2007). Similar to what has been described for apical cilia of NECs (Cohen and Meininger, 1987), a rootlet structure was rarely observed for bl-cilia. The length of the bl-cilia was relatively short (up to 3 μm) and in the same range as that of apical cilia of NECs (Cohen and Meininger, 1987). Together, these observations indicate that bl-cilia share major structural features with apical cilia.

Bl-ciliogenesis at the cell surface

We searched for intermediates in apical and bl-ciliogenesis. Nascent cilia were observed in intracellular vesicles located near, and probably destined for, the ventricular surface (supplementary material Fig. S1G-N), as well as on the apical plasma membrane (Fig. 2A), sometimes apparently just after fusion of an intracellular vesicle (supplementary material Fig. S1O-R). Nascent cilia were also observed on the bl-plasma membrane (Fig. 2B). Likely precursor structures to these were detected in newborn VCs (as indicated by the midbody still being present; Fig. 2C,D); namely, (1) basal bodies tethered directly to the plasma membrane (Fig. 2C) and, albeit less frequently, (2) small chubby cilia in intracellular vesicles that pointed basally and were found basal to AJs (Fig. 2D). Two distinct pathways of ciliogenesis have been described: (1) formation at an intracellular membrane vesicle followed by exocytosis and (2) formation directly at the plasma membrane (Pedersen et al., 2008; Rohatgi and Snell, 2010; Sorokin, 1962; Sorokin, 1968; Sotelo and Trujillo-Cenoz, 1958). Our data are consistent with apical ciliogenesis being initiated predominantly at intracellular vesicles and bl-ciliogenesis predominantly directly at the lateral cell surface.

Ventricular cells with bl-cilia still show apical-basal polarity

We investigated whether the occurrence of bl-cilia reflected the loss of cell polarity and, perhaps, the redistribution of apical membrane constituents to the lateral plasma membrane. Immunogold EM showed that prominin 1 (also known as CD133), which in epithelial cells is a marker of an apical membrane-microdomain (Röper et al., 2000; Weigmann et al., 1997) and found on apical cilia (Dubreuil et al., 2007), was still localized at the apical surface of VCs carrying a bl-cilium (Fig. 2E-H). This apical prominin 1 was observed at the midbody of bl-cilia-forming cells that had just arisen from division (Fig. 2E,F), as is known to be the case for APs forming an apical cilium (Dubreuil et al., 2007), and on the ventricular surface proper of cells bearing a mature bl-cilium (Fig. 2G,H). Similarly, using cholera toxin binding, GM1, a lipid known to be enriched on the apical plasma membrane of epithelial cells

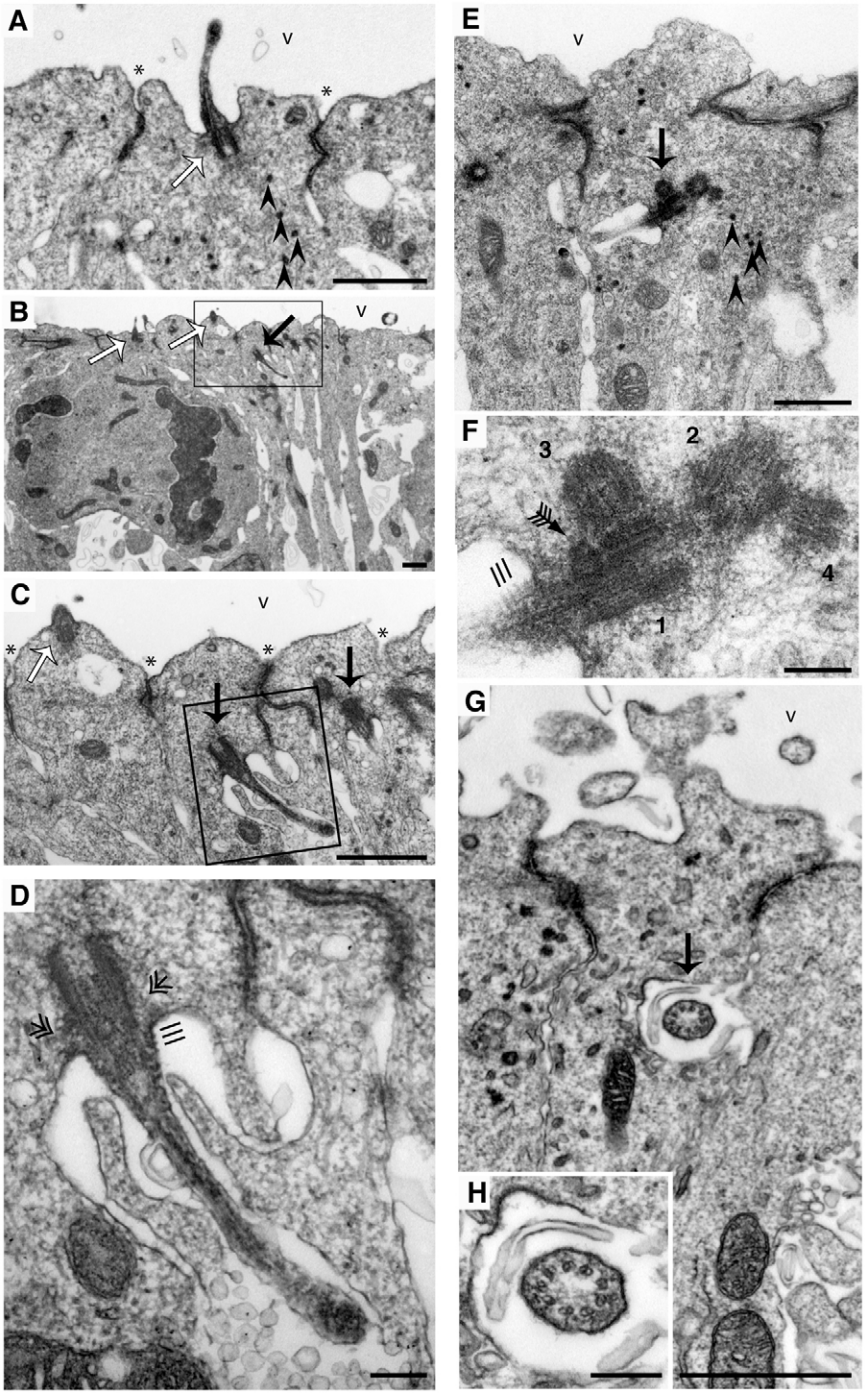

Fig. 1. Mouse NECs exhibit, not only apical, but also bl-cilia. Transmission EM of cilia of VCs in the mouse E12.5-13.5 dTel. (**A-D**) Coexistence of apical cilia (white arrows) protruding into the ventricular lumen (v) and bl-cilia (black arrows) beneath AJs in neighbouring E12.5 VCs. C is a higher magnification of the boxed region in B. D is a higher magnification of the boxed region in C, showing a bl-cilium emanating into the intercellular space. Asterisks, cell boundaries; double-headed arrows, transitional fibres originating from the basal body; triple line, ciliary necklace; arrowheads, centriolar satellites. (**E**,**F**) E13.5 bl-cilium (black arrow) after duplication of centrioles (labelled with 1-4 in F). Feathered arrow, subdistal appendage; triple line, ciliary necklace; arrowheads, some of the centriolar satellites. The tip of the cilium protrudes into the intercellular space (see serial sections in supplementary material Fig. S1). (**G**,**H**) Cross-section of an E12.5 bl-cilium (black arrow) in the intercellular space (higher magnification in H), showing the 9+0 microtubule structure of the axoneme. Ventricular side (v) is up. Scale bars: 1 μm in A-C,E,G; 200 nm in D,F,H.

(Janich and Corbeil, 2007), was largely detected on the ventricular surface and intracellular vesicles beneath it both in VCs with apical cilia (Fig. 2I) and in VCs with bl-cilia (Fig. 2J). Conversely, the bl-membrane protein α6-integrin (Haubst et al., 2006; Wodarz and Huttner, 2003) was still basolateral in both types of VCs (Fig. 2K,L). We conclude that VCs forming bl-cilia still exhibit apical-basal membrane polarity.

Basal bodies of bl-cilia contain Cep164 and Odf2

The switch from apical to bl-ciliogenesis implies a reduced interaction of the post-mitosis centrosome with apical membrane components, an increased interaction with bl-membrane components, or both. There has been significant progress in identifying the molecular players involved in the biogenesis of cilia (Ishikawa and Marshall, 2011; Pedersen et al., 2008; Santos and Reiter, 2008). These include proteins involved in trafficking of nascent cilia to the plasma membrane and in delivery of additional membrane to the growing cilium, as well as proteins associated with transitional fibres and subdistal appendages and, hence, implicated in the interaction of the centrosome with the membrane, such as Cep164 and Odf2 (Dawe et al., 2007; Emmer et al., 2010; Francis et al., 2011; Graser et al., 2007; Ishikawa et al., 2005; Li and Hu, 2011; Pazour and Bloodgood, 2008; Sfakianos et al., 2007). We investigated whether Odf2 and Cep164 are associated with the membrane-tethered basal body of neuroepithelial cilia, and of bl-cilia in particular. Immunogold EM revealed that this was

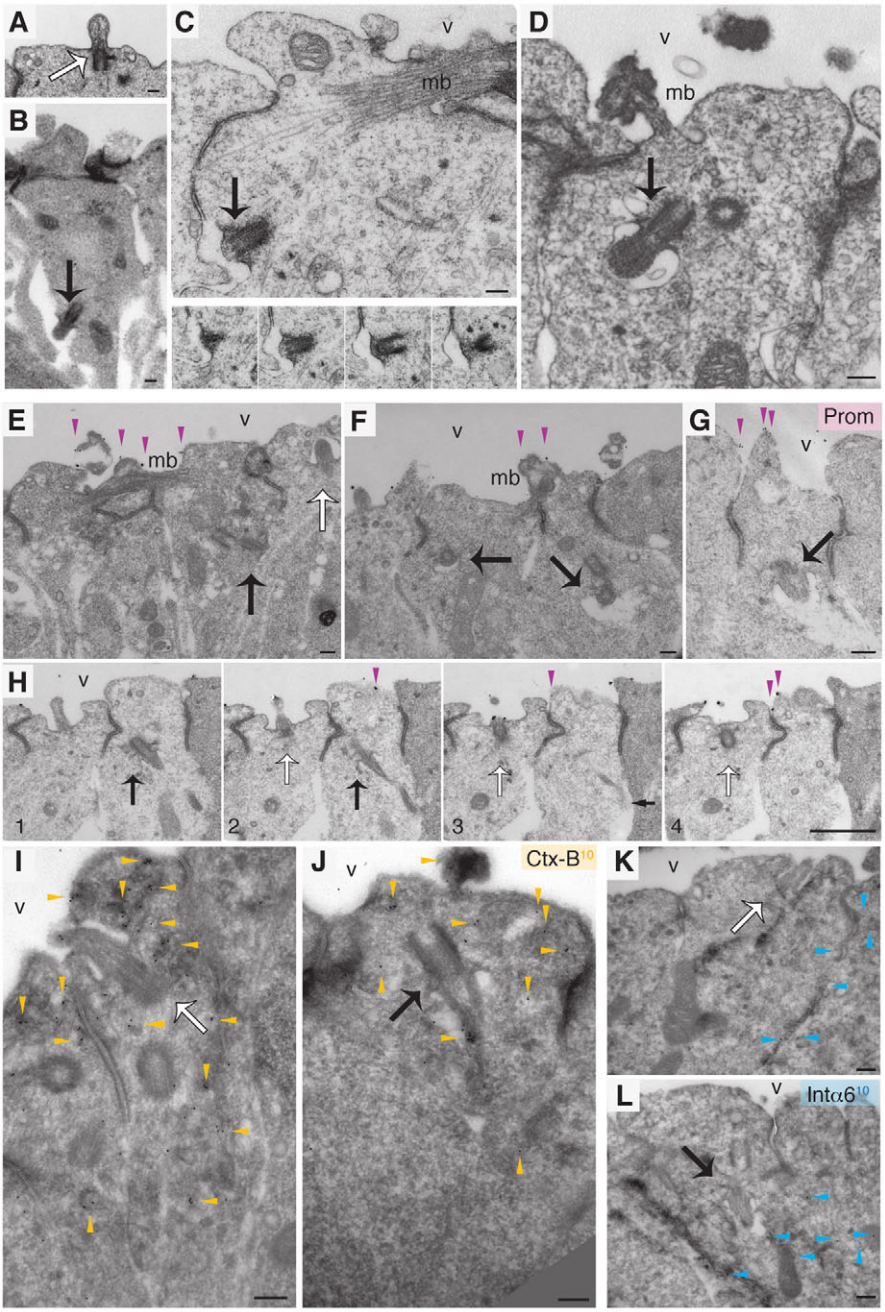

Fig. 2. Ciliogenesis and plasma membrane polarity of bl-cilia-bearing cells.
(**A-D**) Biogenesis of bl-cilia at the plasma membrane and intracellular vesicles of NECs in the mouse E10.5 dTel. Nascent cilia at the apical plasma membrane (A, white arrow), at the bl-plasma membrane (B,C, black arrows) and at an intracellular vesicle (D, black arrow) of VCs. (C) Note that biogenesis of the cilium is initiated at the bl-plasma membrane, as evident from serial sections (insets). (C,D) Note that the cells still exhibit a midbody (mb), implying that ciliogenesis occurred in late telophase/early G1. (**E-L**) Apical-basal plasma membrane polarity of VCs carrying bl-cilia. (E-H) Pre-embedding prominin 1-immunogold labelling of E12.5 (G) and E13.5 (E,F,H) dTel. Cells carrying a bl-cilium (black arrows; nascent in E,F; mature in G-H) show prominin 1 immunoreactivity on the apical midbody (mb; E,F) and the apical plasma membrane (E,G,H) [Prom, silver-enhanced ultrasmall gold (E,F,H), 10-nm gold (G); magenta arrowheads on cells with a bl-cilium]. In an adjacent cell, an apical cilium (H, white arrows) is labelled for prominin 1. (H) Serial sections (1-4). The small black arrow (H, section 3) points to the tip of the bl-cilium in the intercellular space. (I-L) Immunogold-labelled ultrathin frozen sections (10-nm gold) of E13.5 dTel of cells carrying apical (I,K, white arrows) or bl- (K,L, black arrows) cilia. (I,J) Cholera toxin subunit B-Alexa488 (Ctx-B; yellow arrowheads) on apical plasma membrane and in vesicular structures nearby. (K,L) Integrin-α6 (Intα6; blue arrowheads) on bl-plasma membrane. Ventricular side (v) is up. Scale bars: 200 nm in A-G,I-L; 1 μm in H.

indeed the case for both apical and bl-cilia, with immunoreactivity being observed on transitional fibres and, for Odf2 even more so, on the subdistal appendages (supplementary material Fig. S2). These observations suggest that at least some components of the machinery mediating the interaction of the basal body with the membrane are the same for apical and bl-cilia of VCs.

Bl-cilia increase in frequency with progression of neurogenesis

To obtain clues relating to the significance of bl-cilia, we investigated the frequency of their occurrence in the mouse dTel at various stages of neurogenesis (E9.5 to E17.5). Specifically, we determined by EM, in the apical-most ~5-μm region of the VZ, whether mature cilia protruded from the apical surface of NECs (apical cilia) or belonged to the bl-type (see note on terminology in Materials and methods). The latter comprised, in the majority of cases, mature bl-cilia on VCs (although their localization at the cell surface was not corroborated by analysis of serial sections in every single case), with the remainder being cilia on cells that had already delaminated from the AJ belt. Bl-cilia were not observed at E9.5 (Fig. 3), i.e. before the onset of neurogenesis in the dTel (Götz and Huttner, 2005; Kriegstein and Alvarez-Buylla, 2009). Interestingly, bl-cilia appeared at the onset of neurogenesis (E10.5) and their proportion relative to apical cilia increased with the progression of neurogenesis, reaching a value of nearly 50% at E17.5 (Fig. 3). These observations suggested that the appearance of bl-cilia is somehow linked to neurogenesis.

During neurogenesis, APs, in addition to self-renewal, give rise to two further cell types: neurons and BPs (Fietz and Huttner, 2010; Götz and Huttner, 2005; Kriegstein and Alvarez-Buylla, 2009). In

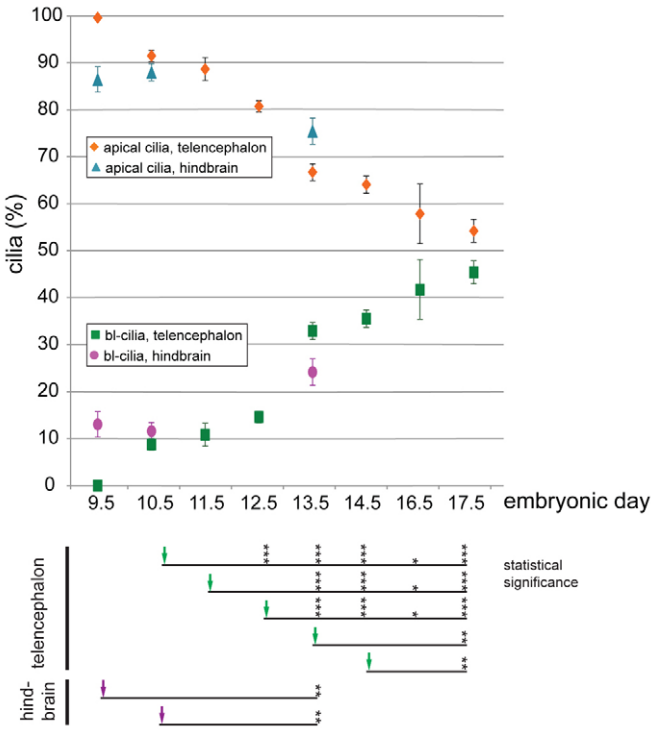

Fig. 3. Bl-cilia and neurogenesis. Bl-cilia increase with progression of neurogenesis. Quantification of mature apical cilia (orange, blue) and bl-type cilia (green, magenta) of cells in the apical-most ~5 μm region of the VZ in mouse dTel (diamonds, squares) and hindbrain (triangles, circles) at the indicated days of embryonic development. Data are expressed as percentage of total cilia (sum of apical plus basolateral) and are the mean of 4-31 different sections (numbers of independent cells analysed are for E9.5-17.5 telencephalon 836, 3161, 1916, 4789, 4022, 6095, 367, 848, and for E9.5-13.5 hindbrain 817, 2996, 541); error bars indicate s.e.m. The statistical significance of the data (*t*-test with Welch's correction) is shown below the graph. Asterisks indicate values significantly different from the reference day (green arrows, telencephalon; magenta arrows, hindbrain); *$P \leq 0.05$; **$P \leq 0.01$; ***$P \leq 0.001$.

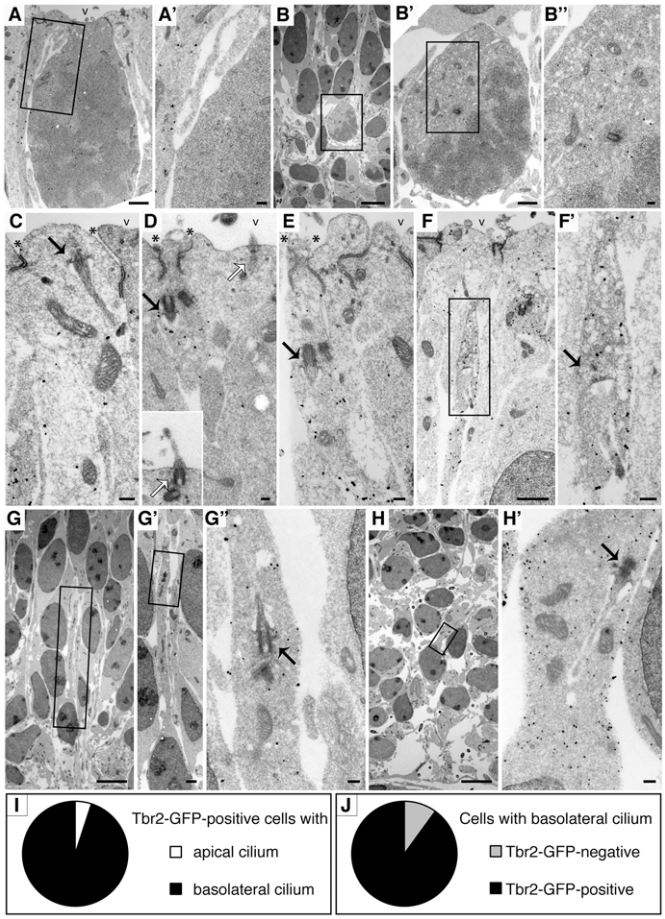

Fig. 4. Bl-cilia are formed by nascent basal progenitors prior to delamination. (A-H′) Pre-embedding GFP-immunogold labelling of E11.5 *Tbr2*-GFP dTel. A′-H′ are higher magnifications of the boxed regions in A-H, respectively. Ventricular side (v) is up. (**A-B″**) Lack of *Tbr2*-GFP immunoreactivity in mitotic AP (A,A′) and its presence in a mitotic BP in the arising SVZ (B-B″). Note the *Tbr2*-GFP immunoreactivity in the interphase cell adjacent to the mitotic AP in (A,A′). (**C-F′**) Bl-cilia (black arrows) of *Tbr2*-GFP-positive interphase cells in the VZ, i.e. of nascent BPs. Note the presence of apical AJs and apical plasma membrane, and the increasing apical constriction, in the nascent BPs in C-E. Asterisks, cell boundaries. The nascent BP in D is adjacent to a *Tbr2*-GFP-negative interphase AP with an apical cilium (white arrow), a consecutive section of which is shown in the inset; see also supplementary material Fig. S3. (**G-H′**) Cilia (black arrows) in a *Tbr2*-GFP-positive BP in the arising SVZ (G-G″) and a neuron in the preplate (H,H′). Basal lamina is near the bottom in H. Scale bars: 5 μm in B,G,H; 1 μm in A,B′,F,G′; 200 nm in A′,B″,C-E,F′,G″,H′. (**I**,**J**) Quantification of apical and bl-cilia on *Tbr2*-GFP-positive VCs (I), and of *Tbr2*-GFP-positive and -negative VCs carrying bl-cilia (J). The data shown are estimates based on at least 20 *Tbr2*-GFP-positive VCs analysed.

the dTel, the progeny of neurogenic APs are mostly BPs, whereas in the hindbrain almost all are neurons (Haubensak et al., 2004). Neurogenesis in the hindbrain starts earlier than in the dTel, and the increase in neuron-generating APs over time is less steep than in the cortex (Götz and Huttner, 2005; Haubensak et al., 2004). Consistent with a link between the appearance of bl-cilia and neurogenesis, we observed, in the apical-most ~5-μm region of the hindbrain VZ, bl-type cilia already at E9.5, and the increase in their proportion from E10.5 to E13.5 was less steep than that in the dTel (Fig. 3). These data provided further support for the notion that the appearance of bl-cilia is linked to the generation of BPs and neurons from APs.

dTel ventricular cells with bl-cilia are nascent BPs

Newborn neurons and BPs initially might still be in contact with the ventricle and be integrated into the AJ belt, from which they subsequently delaminate (Fietz and Huttner, 2010; Konno et al., 2008; Kriegstein and Alvarez-Buylla, 2009). We therefore explored whether the cells with apical plasma membrane, apical AJs and a bl-cilium observed in the E12.5-13.5 dTel (Fig. 1) were nascent BPs. For this purpose, we made use of a mouse line expressing cytosolic GFP under the control of the promoter of Tbr2 (Gong et al., 2003; Kwon and Hadjantonakis, 2007), a transcription factor specifically expressed in BPs of dTel (Englund et al., 2005). Importantly, nascent BPs can initiate Tbr2 expression when they are still located at, or near, the ventricular surface (Kowalczyk et al., 2009).

Pre-embedding immunogold labelling for GFP followed by EM revealed immunoreactivity indicative of Tbr2 expression in the cytoplasm of mitotic cells located at the basal boundary of the VZ (mitotic BPs), but not of apical mitotic cells (mitotic APs), as

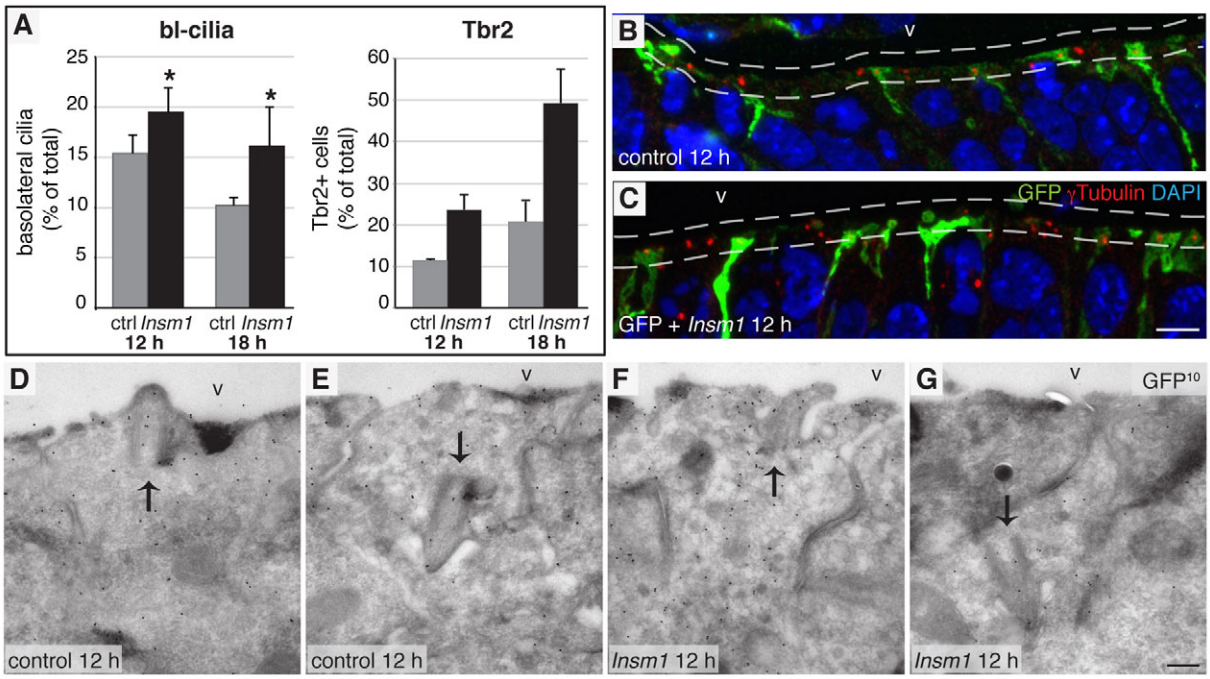

Fig. 5. Increased proportion of bl-cilia upon *Insm1* overexpression. dTel of E12.5 mouse embryos was subjected to in utero electroporation with *GFP* (control) or *GFP+Insm1* (*Insm1*) plasmids, and was analysed 12 and 18 hours later. (**A**) Quantification of bl-cilia in GFP-positive cells in the apical-most region of the VZ [left, expressed as percentage of total (sum of apical plus bl-cilia)], and of Tbr2-positive (Tbr2+) cells in VZ and SVZ (right, expressed as percentage of total GFP-positive cells), in control- (grey columns) and *Insm1*- (black columns) transfected VCs. Data are the mean of three (bl-cilia) and two (Tbr2) counts; error bars indicate s.d. (bl-cilia) or the variation of values from the mean (Tbr2). **P*<0.05 (unpaired, one-tailed *t*-test; 12 hours, *P*=0.04; 18 hours, *P*=0.03). (**B**,**C**) Double immunofluorescence for GFP (green) and γ-tubulin (red) on 150 nm-thick frozen sections of control- (A) and *Insm1*- (B) transfected VZ. Dashed lines indicate the apical-most region analysed for apical and bl-cilia in GFP-positive cells. (**D-G**) Immunogold (GFP, 10 nm) EM of ultrathin frozen sections of control- (D,E) and *Insm1*- (F,G) transfected VCs. Arrows indicate apical (D,F) and bl- (E,G) cilia in GFP-positive cells. v, ventricle. Scale bars: 5 μm in C (for B,C); 200 nm in G (for D-G).

expected (Fig. 4A-B″). Few non-mitotic cells with ventricular contact showed *Tbr2*-GFP immunoreactivity (Fig. 4C-E). Remarkably, in >95% of the cases in which a cilium was contained in the ultrathin section of such an immunolabelled VC, it was localized basolaterally (Fig. 4I). This indicated that nascent BPs, which still exhibit ventricular contact and integration into the AJ belt and thus have not yet undergone delamination, place their cilium on the basolateral rather than apical plasma membrane. This constitutes a major difference to the APs from which BPs arise, which carry apical cilia (Fig. 4D, inset). Furthermore, ~90% of the VCs with bl-cilia were *Tbr2*-GFP-positive, although in some cases the level of immunoreactivity was low (Fig. 4C,J). This implies that a transcriptional programme characteristic of BPs is initiated by the time that a bl-cilium is formed in AP progeny.

In many (Fig. 4D,E; supplementary material Fig. S3), but not all (Fig. 4C), instances, the width between the apical AJs (as observed in ultrathin sections) was less in the *Tbr2*-GFP-positive, bl-cilia-carrying VCs than in the *Tbr2*-GFP-negative, apical cilia-carrying APs. This indicates that the formation of a bl-cilium in nascent, still ventricular, BPs precedes apical constriction, which in turn precedes their delamination. Accordingly, *Tbr2*-GFP-positive cells lacking ventricular contact exhibited cilia emerging from what corresponded to the previous bl-membrane (Fig. 4F,F′). These cells were BPs that had delaminated from the AJ belt but the nuclei of which were still located in the VZ. The cilia of these delaminated BPs were typically found on the retracting apical process rather than in the vicinity of the cell body (Fig. 4F). Similarly, cilia were also observed on *Tbr2*-GFP-positive BPs that had further delaminated in that their nuclei were located in the SVZ (Fig. 4G-G″). Here, the cilium was typically observed closer to (Fig. 4G′), or even on (data not shown), the cell body. In line with previous observations (Lee and Gleeson, 2010; Louvi and Grove, 2011), the newborn neurons that had inherited *Tbr2*-GFP from their BP mothers (Kowalczyk et al., 2009; Kwon and Hadjantonakis, 2007) and had migrated from the SVZ basally to form the developing cortical plate, showed cilia that, in most cases, emerged from a plasma membrane pocket close to their nucleus (Fig. 4H,H′).

Insm1 overexpression increases bl-cilia

Given that in the VZ of the dTel, cells with bl-cilia are predominately nascent BPs, we investigated whether conditions leading to increased delamination of BPs also increased bl-cilia. We addressed this issue by overexpression of the transcription factor insulinoma-associated 1 (*Insm1*), which promotes the generation of BPs from APs (Farkas et al., 2008) (Fig. 5A). Specifically, we determined the occurrence of apical and bl-cilia in control- (*GFP* only) and *Insm1*- (*Insm1+GFP*) transfected cells in the apical-most region of the VZ (Fig. 5B,C) 12 and 18 hours after in utero electroporation of the dTel of E12.5 embryos, using immunogold labelling of ultrathin cryosections for GFP to identify transfected VCs (Fig. 5D-G). *Insm1* overexpression caused a significant increase in the proportion of VCs with bl-cilia (Fig. 5A). As most of these cells constituted daughter

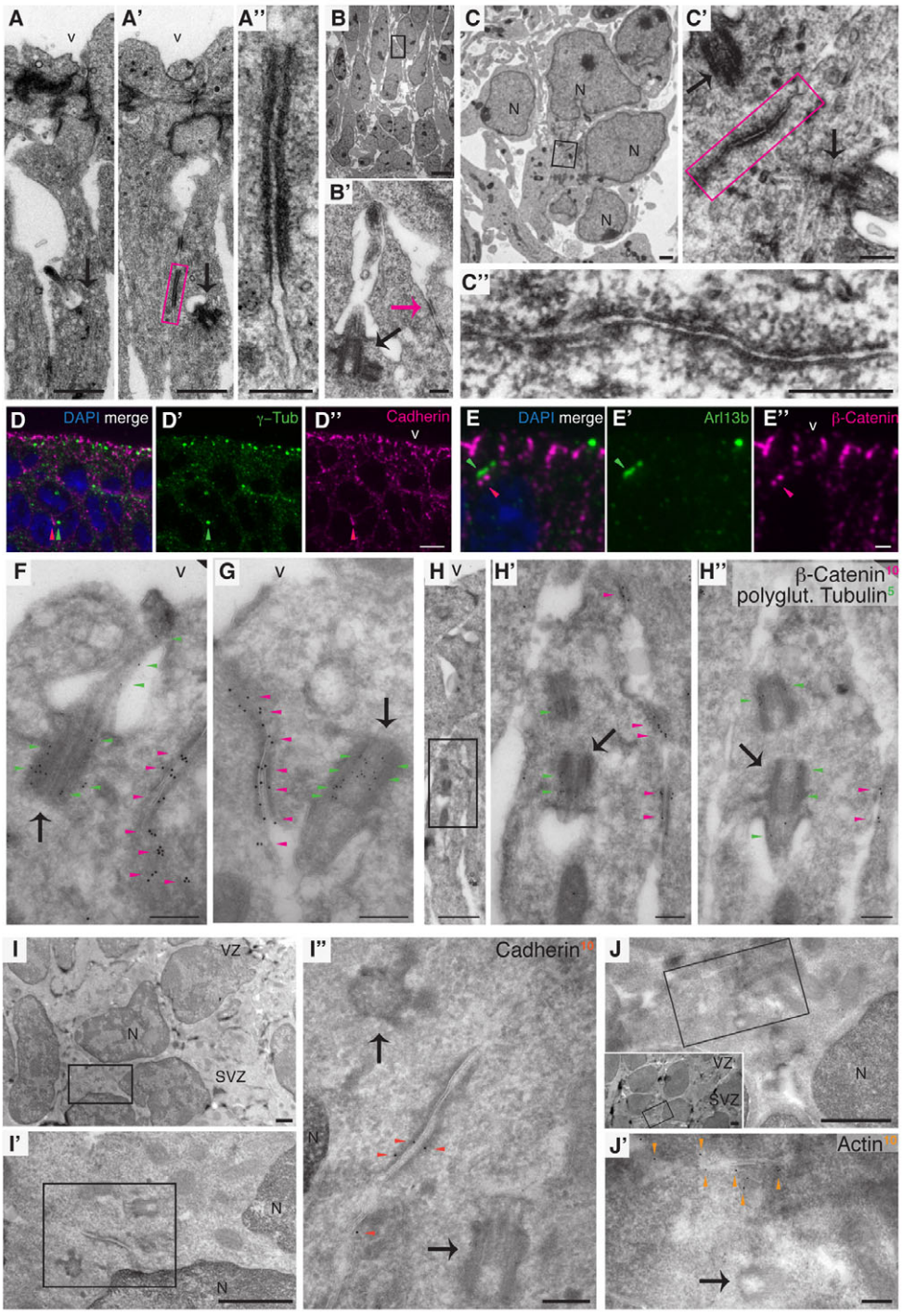

Fig. 6. Cilia of delaminated BPs and neurons are preferentially located adjacent to spot-like AJs. (**A-C″**) EM of E12.5 (C-C″) and 13.5 (A-B′) mouse dTel showing the proximity of cilia (black arrows) and junctional complexes (magenta boxes and arrow) in a presumptive nascent BP in the VZ (A-A″), a probably delaminated BP in the SVZ (B,B′) and neurons in the preplate (C-C″). (A,A′) Serial sections; see also supplementary material Fig. S4A-F. (**D-E″**) Double immunofluorescence for γ-tubulin (green) and cadherin (magenta) (D-D″), and for Arl13b (green) and β-catenin (magenta) (E-E″), combined with DAPI staining (blue), on ultrathin (150 nm) frozen sections of E12.5-13.5 dTel. Note the centrosome (green arrowheads in D,D′) adjacent to a spot-like AJ (magenta arrowheads in D,D″) in the region basal to the apical-most nuclear layer (D-D″), and the cilium (green arrowheads in E,E′) adjacent to a spot-like AJ (magenta arrowheads in E,E″) close to, but not integrated into, the apical adherens belt (E-E″). (**F-J′**) EM of ultrathin frozen sections of E13.5 dTel double-immunogold-labelled for β-catenin and polyglutamylated tubulin (F-H″; β-catenin: 10-nm-gold, magenta arrowheads; polyglutamylated tubulin: 5-nm-gold, green arrowheads), or immunogold-labelled for cadherin (I-I″; 10-nm-gold, red arrowheads) or actin (J,J′; 10-nm-gold, orange arrowheads). Box in inset in J indicates the region shown in J. Note the basal-bodies/centrioles near β-catenin- or cadherin-labelled AJs in (F,G,H′,H″,I″, arrows), and the centriole near an actin-labelled AJ in (J′, arrow). H′ and H″ are consecutive sections. Micrographs in F,G are at the ventricular surface; H-H″ in the VZ; I-I″,J,J′ in the SVZ. H′-J′ are higher magnifications of the boxed regions in H-J, respectively. N, nucleus. Ventricular side (v) is up. Scale bars: 5 μm in B,D″ (for D-D″); 1 μm in A,A′,C,E″ (for E-E″),H,I,I′,J (+inset); 200 nm in A″,B′,C′,C″,F,G,H′,H″,I″,J′.

cells of transfected APs that re-established a cilium after mitosis, we conclude that establishing a cilium on the bl-plasma membrane precedes the increased delamination of VCs to become BPs in response to *Insm1* overexpression.

Cilia of BPs and neurons are adjacent to spot-like AJs

What are the cues that direct bl-cilia and cilia of delaminated BPs and neurons to specific sites of the plasma membrane? We noticed that bl-cilia were not randomly distributed along the bl-plasma membrane, but that the majority was found just basal to the AJ belt (Fig. 1C,E,G). Furthermore, we observed that apical cilia (as judged from their basal bodies/centrioles) were largely centred with respect to the AJ belt (supplementary material Fig. S4G). These data raised the possibility that junctional components such as cadherins might be involved in cilia positioning. Of relevance for bl-cilia positioning, cadherins are not confined to apical AJs but are known to occur throughout the cortical wall (Kadowaki et al., 2007; Marthiens and ffrench-Constant, 2009). This reflects puncta adhaerentia (Hinds and Ruffett, 1971), which are spot-like AJs along the bl-plasma membrane of VCs and on the plasma membrane of delaminated BPs and neurons.

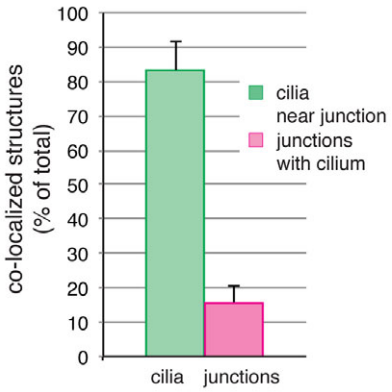

Fig. 7. Quantification of the colocalization of cilia and spot-like AJs. Bl-cilia and spot-like AJs basally to the apical AJ belt in the VZ of E13.5 mouse dTel were quantified on immunogold-labelled ultrathin frozen sections as shown in Fig. 6H-H″. Bl-cilia near spot-like AJs are expressed as percentage of total bl-cilia (green column), and spot-like AJs with a cilium in their vicinity as percentage of total spot-like AJs (magenta column). Data are the mean of nine sections; error bars indicate s.e.m.

We therefore investigated a possible spatial relationship between bl-type cilia and spot-like AJs. Indeed, EM revealed bl-cilia of VCs, and cilia of delaminated BPs and neurons, in the vicinity of electron-dense plaques that resembled AJs (Fig. 6A-C″; supplementary material Fig. S4A-F). The identity of these junctions as spot-like AJs was corroborated by double immunofluorescence on ultrathin frozen sections for cadherin and the centrosomal marker γ-tubulin (Fig. 6D-D″), or for β-catenin and the ciliary membrane marker Arl13b (Fig. 6E-E″), by double-immunogold EM for β-catenin and polyglutamylated tubulin, another marker of cilia (Hammond et al., 2008; Sloboda, 2009) (Fig. 6H-H″), and by immunogold EM for cadherin (Fig. 6I-I″) and actin (Fig. 6J,J′). In accordance with these observations on embryonic mouse cerebral cortex, in the SVZ of foetal human cerebral cortex, centrosomes were found to be located close to spot-like AJs (supplementary material Fig. S4H-L).

We quantified and statistically tested the spatial relationship between AJs and bl-cilia (for an example, see supplementary material Fig. S5). Indeed, EM analysis of the VZ of E13.5 dTel revealed that >80% of the bl-cilia of cells that had probably delaminated from the apical AJ belt were found in the vicinity (within 500 nm) of spot-like AJs, which on average were six per cell (Fig. 7). This frequency of colocalization of bl-cilia and spot-like AJs was much greater than would be expected if bl-cilia were randomly distributed with respect to spot-like AJs, the probability in the latter case being 1 in 22 (Table 1). We conclude that the occurrence of bl-cilia in the vicinity of spot-like AJs is highly significant and suggests a role of spot-like AJs in the positioning of bl-cilia.

DISCUSSION

The present results uncover a novel cell biological feature of newborn NECs destined to change fate, that is, to delaminate from the apical AJ belt: the re-establishing of their primary cilium at the basolateral, rather than apical, plasma membrane (Fig. 8). Our finding that virtually all *Tbr2*-GFP-positive VCs (i.e. nascent BPs) exhibit a bl-cilium indicates that re-establishing the cilium at the bl-plasma membrane constitutes an obligatory step in their delamination process. This conclusion is not contradicted by the existence of a few *Tbr2*-GFP-negative VCs with bl-cilia, as these were probably either nascent BPs that had not yet started to express *Tbr2*-GFP to a detectable level, or nascent neurons (which do not express Tbr2) (Englund et al., 2005). The appearance of bl-cilia with the onset, and their increase in abundance with the progression, of neurogenesis are consistent with the notion that formation of a bl-cilium is a hallmark of delamination.

Interestingly, re-establishing of the cilium at the bl-plasma membrane preceded the actual delamination step, i.e. it occurred in cells that were still integrated into the AJ belt and exhibited apical-basal polarity, reflected, in particular, by the presence of apical plasma membrane (Fig. 8). Importantly, the increased delamination of BPs upon overexpression of *Insm1* (Farkas et al., 2008) was preceded by increased formation of bl-cilia, providing strong support for a link between bl-ciliogenesis and BP delamination. A bl-cilium thus emerges as the earliest cell biological feature described to date that is observed specifically in those VCs that delaminate from the apical AJ belt to become BPs or neurons. Although the latter cells do not transgress the basal lamina but remain within the tissue corresponding to the original neuroepithelium, it will be interesting to investigate whether re-establishing the cilium at the basolateral rather than apical plasma membrane also occurs when cells delaminate from an epithelium, including transgression of the basal lamina; for example, in the formation of the neural crest from the neural plate (Acloque et al., 2009; Hay, 2005) or of the endocrine pancreas from the endoderm (Cole et al., 2009; Rukstalis and Habener, 2007). On a more general note, the question arises whether bl-ciliogenesis is a common feature of epithelial-mesenchymal transition and whether it could be involved in cancer metastasis.

Although the mechanism underlying bl-ciliogenesis remains to be investigated further, the statistically highly significant occurrence of bl-cilia in the vicinity of spot-like AJs suggests a role of the latter in the positioning of bl-cilia (Fig. 8; supplementary material Fig. S6). Such a role would be consistent with previous data obtained in other systems showing a spatial relationship between centrosomes and AJs (Bornens, 2008; Dupin et al., 2009). It might also be interesting to explore whether Lkb1 (Stk11 – Mouse Genome Informatics) might be involved in ciliary positioning in NECs as this protein kinase has been found to

Table 1. Probability of colocalization of randomly distributed bl-cilium and spot-like AJs in the VZ

Radial thickness of VZ (μm)*	Minimum length of lateral membrane (μm)‡	Average number of spot-like AJs per VZ cell§	Average number of per spot-like AJs per lateral membrane§	Maximum size of bl-cilium/spot-like AJ assembly (μm)	Probability of colocalization¶
85±4	83	6.3	3.15	1.2	$P \leq 0.045 = \leq 1:22$

Data were obtained from, and refer to, EM sections.
*Mean of 14 sections ± s.d.
‡Deduced by subtracting the maximum thickness of the AJ belt (2 μm) from the average thickness of the VZ.
§The average number of spot-like AJs per VZ cell was calculated using the data shown in Fig. 7, based on the occurrence of one primary cilium per cell; the average number of spot-like AJs per lateral membrane is half this value.
¶Probability was calculated according to $P=1-(1-1.2/83)^{3.15}$.

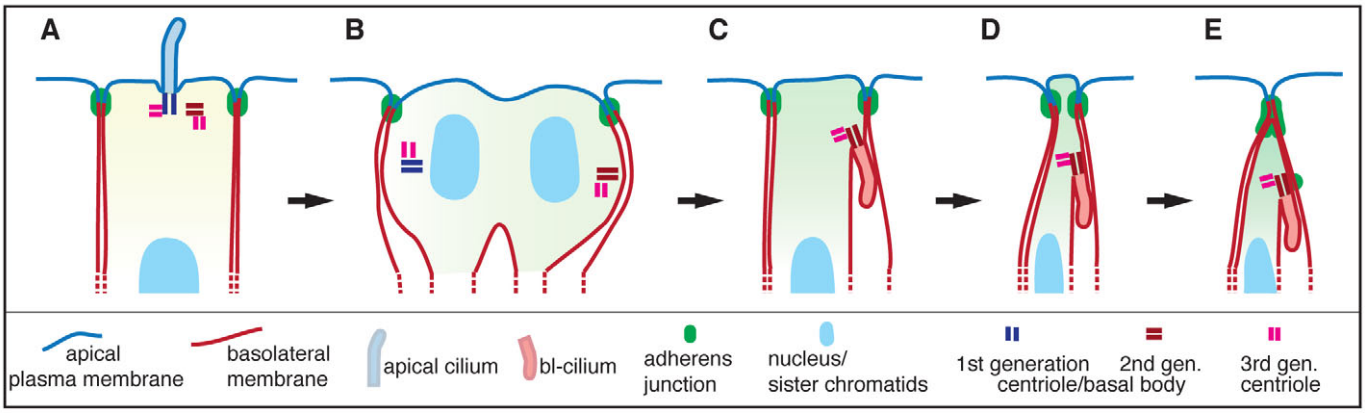

Fig. 8. Bl-cilia and neural progenitor delamination. Cartoon illustrating the formation of a bl-cilium after AP mitosis, which precedes apical constriction and delamination. An AP with an apical cilium (**A**) undergoes mitosis (**B**). The daughter cell inheriting the younger centrosome forms a bl-cilium while still being integrated in the apical junctional belt (**C**), followed by apical constriction (**D**) resulting in loss of apical plasma membrane, formation of spot-like AJs and delamination (**E**).

influence the location of the cilium with regard to plasma membrane domains, albeit in pancreatic β-cells, which do not exhibit proper apical-basal polarity (Granot et al., 2009).

The present observation of a bl-cilium in nascent BPs and neurons has intriguing implications for centrosome inheritance. In the course of centrosome duplication during the cell cycle, the cilium's basal body and its associated second centriole, i.e. the older ('first generation') and younger ('second generation') centriole, respectively, dissociate from one another, with each ending up, together with the newly synthesized ('third generation') centrioles, in one of the two centrosomes (Bettencourt-Dias and Glover, 2007; Nigg and Raff, 2009) (Fig. 8). It has recently been shown that upon AP asymmetric division, the centrosome containing the first-generation centriole is preferentially found in the daughter cell remaining an AP and the centrosome containing the second-generation centriole in the progeny that delaminates and eventually becomes a neuron (Wang et al., 2009). This implies (at least in mouse) that the first-generation centriole becomes the basal body of the apical cilium of the daughter AP, and the second-generation centriole the basal body of the bl-cilium of the nascent daughter BP/neuron. Extrapolating from observations with 3T3 cells in culture (Anderson and Stearns, 2009), this in turn may imply that the daughter AP grows its cilium earlier than the daughter BP/neuron.

Given that cilia are key sensory organelles (Berbari et al., 2009; Goetz and Anderson, 2010; Lancaster and Gleeson, 2009), our finding of bl-cilia on subsequently delaminating BPs/neurons has intriguing implications with regard to signalling. Apical cilia are in a strategic location to sense signals specifically present in the ventricular fluid, whereas bl-cilia are not. Re-establishing the cilium at the bl-plasma membrane may thus deprive VCs of sensing a ventricular signal. Instead, bl-cilia might allow sensing signals originating from the lateral plasma membrane of neighbouring NECs or those present in the intercellular space. Such alteration in signalling could promote the cell fate changes associated with the transition from APs to BPs and neurons, including delamination. In addition, with regard to spatial constraints and cytoskeletal organization, re-establishing the cilium at the basolateral rather than apical plasma membrane might be an advantage, if not a prerequisite, for constriction of the apical-most region of a VC for subsequent delamination.

Importantly, the appearance of neural progenitors that delaminate from the apical AJ belt to form the SVZ, notably the outer SVZ, is thought to be a crucial step in the expansion of the cerebral cortex during mammalian, and in particular primate, evolution (Fietz et al., 2010; Hansen et al., 2010; Reillo et al., 2011). Thus, re-establishing the cilium at the basolateral rather than apical plasma membrane of a VC that retains mitotic activity might turn out to be a cellular biological step that is at the core of cortical expansion.

Acknowledgements

We thank Dr Robert Hevner for kindly providing the *Tbr2*-GFP mouse line; Drs Johannes Vogt (Charite, Berlin) and Simone Fietz for human foetal tissue; Katja Langenfeld for excellent technical assistance; Drs Yannis Kalaidzidis and Andreas Ettinger for help with statistics; Jussi Helppi and other members of the animal facility, and the electron microscopy facility, of the Max Planck Institute of Molecular Cell Biology and Genetics for excellent support; and Dr Caren Norden for helpful comments on the manuscript.

Funding

This work was supported by a European Molecular Biology Organization (EMBO) long-term-fellowship [to J.T.M.L.P.]; grants from the German Research Foundation (DFG) [SFB 655, A2 and TRR 83, Tp6 to W.B.H.]; a grant from the European Research Council (ERC) [250197 to W.B.H.]; the DFG-funded Center for Regenerative Therapies Dresden; and the Fonds der Chemischen Industrie.

Competing interests statement

The authors declare no competing financial interests.

Supplementary material

Supplementary material available online at
http://dev.biologists.org/lookup/suppl/doi:10.1242/dev.069294/-/DC1

References

Acloque, H., Adams, M. S., Fishwick, K., Bronner-Fraser, M. and Nieto, M. A. (2009). Epithelial-mesenchymal transitions: the importance of changing cell state in development and disease. *J. Clin. Invest.* **119**, 1438-1449.

Anderson, C. T. and Stearns, T. (2009). Centriole age underlies asynchronous primary cilium growth in mammalian cells. *Curr. Biol.* **19**, 1498-1502.

Berbari, N. F., O'Connor, A. K., Haycraft, C. J. and Yoder, B. K. (2009). The primary cilium as a complex signaling center. *Curr. Biol.* **19**, R526-R535.

Bettencourt-Dias, M. and Glover, D. M. (2007). Centrosome biogenesis and function: centrosomics brings new understanding. *Nat. Rev. Mol. Cell. Biol.* **8**, 451-463.

Bornens, M. (2008). Organelle positioning and cell polarity. *Nat. Rev. Mol. Cell. Biol.* **9**, 874-886.

Cohen, E. and Meininger, V. (1987). Ultrastructural analysis of primary cilium in the embryonic nervous tissue of mouse. *Int. J. Dev. Neurosci.* **5**, 43-51.

Cole, L., Anderson, M., Antin, P. B. and Limesand, S. W. (2009). One process for pancreatic beta-cell coalescence into islets involves an epithelial-mesenchymal transition. *J. Endocrinol.* **203**, 19-31.
Dawe, H. R., Farr, H. and Gull, K. (2007). Centriole/basal body morphogenesis and migration during ciliogenesis in animal cells. *J. Cell Sci.* **120**, 7-15.
Dubreuil, V., Marzesco, A. M., Corbeil, D., Huttner, W. B. and Wilsch-Brauninger, M. (2007). Midbody and primary cilium of neural progenitors release extracellular membrane particles enriched in the stem cell marker prominin-1. *J. Cell Biol.* **176**, 483-495.
Dupin, I., Camand, E. and Etienne-Manneville, S. (2009). Classical cadherins control nucleus and centrosome position and cell polarity. *J. Cell Biol.* **185**, 779-786.
Emmer, B. T., Maric, D. and Engman, D. M. (2010). Molecular mechanisms of protein and lipid targeting to ciliary membranes. *J. Cell Sci.* **123**, 529-536.
Englund, C., Fink, A., Lau, C., Pham, D., Daza, R. A., Bulfone, A., Kowalczyk, T. and Hevner, R. F. (2005). Pax6, Tbr2, and Tbr1 are expressed sequentially by radial glia, intermediate progenitor cells, and postmitotic neurons in developing neocortex. *J. Neurosci.* **25**, 247-251.
Farkas, L. M. and Huttner, W. B. (2008). The cell biology of neural stem and progenitor cells and its significance for their proliferation versus differentiation during mammalian brain development. *Curr. Opin. Cell Biol.* **20**, 707-715.
Farkas, L. M., Haffner, C., Giger, T., Khaitovich, P., Nowick, K., Birchmeier, C., Paabo, S. and Huttner, W. B. (2008). Insulinoma-associated 1 has a panneurogenic role and promotes the generation and expansion of basal progenitors in the developing mouse neocortex. *Neuron* **60**, 40-55.
Fietz, S. A. and Huttner, W. B. (2010). Cortical progenitor expansion, self-renewal and neurogenesis-a polarized perspective. *Curr. Opin. Neurobiol.* **21**, 23-35.
Fietz, S. A., Kelava, I., Vogt, J., Wilsch-Bräuninger, M., Stenzel, D., Fish, J. L., Corbeil, D., Riehn, A., Distler, W., Nitsch, R. et al. (2010). OSVZ progenitors of human and ferret neocortex are epithelial-like and expand by integrin signaling. *Nat. Neurosci.* **13**, 690-699.
Francis, S. S., Sfakianos, J., Lo, B. and Mellman, I. (2011). A hierarchy of signals regulates entry of membrane proteins into the ciliary membrane domain in epithelial cells. *J. Cell Biol.* **193**, 219-233.
Goetz, S. C. and Anderson, K. V. (2010). The primary cilium: a signalling centre during vertebrate development. *Nat. Rev. Genet.* **11**, 331-344.
Gong, S., Zheng, C., Doughty, M. L., Losos, K., Didkovsky, N., Schambra, U. B., Nowak, N. J., Joyner, A., Leblanc, G., Hatten, M. E. et al. (2003). A gene expression atlas of the central nervous system based on bacterial artificial chromosomes. *Nature* **425**, 917-925.
Götz, M. and Huttner, W. B. (2005). The cell biology of neurogenesis. *Nat. Rev. Mol. Cell. Biol.* **6**, 777-788.
Granot, Z., Swisa, A., Magenheim, J., Stolovich-Rain, M., Fujimoto, W., Manduchi, E., Miki, T., Lennerz, J. K., Stoeckert, C. J., Jr, Meyuhas, O. et al. (2009). LKB1 regulates pancreatic beta cell size, polarity, and function. *Cell Metab.* **10**, 296-308.
Graser, S., Stierhof, Y. D., Lavoie, S. B., Gassner, O. S., Lamla, S., Le Clech, M. and Nigg, E. A. (2007). Cep164, a novel centriole appendage protein required for primary cilium formation. *J. Cell Biol.* **179**, 321-330.
Hammond, J. W., Cai, D. and Verhey, K. J. (2008). Tubulin modifications and their cellular functions. *Curr. Opin. Cell Biol.* **20**, 71-76.
Han, Y. G. and Alvarez-Buylla, A. (2010). Role of primary cilia in brain development and cancer. *Curr. Opin. Neurobiol.* **20**, 58-67.
Hansen, D. V., Lui, J. H., Parker, P. R. and Kriegstein, A. R. (2010). Neurogenic radial glia in the outer subventricular zone of human neocortex. *Nature* **464**, 554-561.
Haubensak, W., Attardo, A., Denk, W. and Huttner, W. B. (2004). Neurons arise in the basal neuroepithelium of the early mammalian telencephalon: A major site of neurogenesis. *Proc. Natl. Acad. Sci. USA* **101**, 3196-3201.
Haubst, N., Georges-Labouesse, E., De Arcangelis, A., Mayer, U. and Gotz, M. (2006). Basement membrane attachment is dispensable for radial glial cell fate and for proliferation, but affects positioning of neuronal subtypes. *Development* **133**, 3245-3254.
Hay, E. D. (2005). The mesenchymal cell, its role in the embryo, and the remarkable signaling mechanisms that create it. *Dev. Dyn.* **233**, 706-720.
Hinds, J. W. and Ruffett, T. L. (1971). Cell proliferation in the neural tube: An electron microscopic and Golgi analysis in the mouse cerebral vesicle. *Z. Zellforsch. Mikrosk. Anat.* **115**, 226-264.
Ishikawa, H. and Marshall, W. F. (2011). Ciliogenesis: building the cell's antenna. *Nat. Rev. Mol. Cell. Biol.* **12**, 222-234.
Ishikawa, H., Kubo, A. and Tsukita, S. (2005). Odf2-deficient mother centrioles lack distal/subdistal appendages and the ability to generate primary cilia. *Nat. Cell Biol.* **7**, 517-524.
Janich, P. and Corbeil, D. (2007). GM1 and GM3 gangliosides highlight distinct lipid microdomains within the apical domain of epithelial cells. *FEBS Lett.* **581**, 1783-1787.
Kadowaki, M., Nakamura, S., Machon, O., Krauss, S., Radice, G. L. and Takeichi, M. (2007). N-cadherin mediates cortical organization in the mouse brain. *Dev. Biol.* **304**, 22-33.
Konno, D., Shioi, G., Shitamukai, A., Mori, A., Kiyonari, H., Miyata, T. and Matsuzaki, F. (2008). Neuroepithelial progenitors undergo LGN-dependent planar divisions to maintain self-renewability during mammalian neurogenesis. *Nat. Cell Biol.* **10**, 93-101.
Kowalczyk, T., Pontious, A., Englund, C., Daza, R. A., Bedogni, F., Hodge, R., Attardo, A., Bell, C., Huttner, W. B. and Hevner, R. F. (2009). Intermediate neuronal progenitors (basal progenitors) produce pyramidal-projection neurons for all layers of cerebral cortex. *Cereb. Cortex* **19**, 2439-2450.
Kriegstein, A. and Alvarez-Buylla, A. (2009). The glial nature of embryonic and adult neural stem cells. *Annu. Rev. Neurosci.* **32**, 149-184.
Kwon, G. S. and Hadjantonakis, A. K. (2007). Eomes::GFP-a tool for live imaging cells of the trophoblast, primitive streak, and telencephalon in the mouse embryo. *Genesis* **45**, 208-217.
Lancaster, M. A. and Gleeson, J. G. (2009). The primary cilium as a cellular signaling center: lessons from disease. *Curr. Opin. Genet. Dev.* **19**, 220-229.
Lee, J. H. and Gleeson, J. G. (2010). The role of primary cilia in neuronal function. *Neurobiol. Dis.* **38**, 167-172.
Li, Y. and Hu, J. (2011). Small GTPases and cilia. *Protein Cell* **2**, 13-25.
Louvi, A. and Grove, E. A. (2011). Cilia in the CNS: the quiet organelle claims center stage. *Neuron* **69**, 1046-1060.
Marshall, W. F. (2008). Basal bodies platforms for building cilia. *Curr. Top. Dev. Biol.* **85**, 1-22.
Marthiens, V. and ffrench-Constant, C. (2009). Adherens junction domains are split by asymmetric division of embryonic neural stem cells. *EMBO Rep.* **10**, 515-520.
Nigg, E. A. and Raff, J. W. (2009). Centrioles, centrosomes, and cilia in health and disease. *Cell* **139**, 663-678.
Pazour, G. J. and Bloodgood, R. A. (2008). Targeting proteins to the ciliary membrane. *Curr. Top. Dev. Biol.* **85**, 115-149.
Pedersen, L. B., Veland, I. R., Schroder, J. M. and Christensen, S. T. (2008). Assembly of primary cilia. *Dev. Dyn.* **237**, 1993-2006.
Reillo, I., de Juan Romero, C., Garcia-Cabezas, M. A. and Borrell, V. (2011). A role for intermediate radial glia in the tangential expansion of the mammalian cerebral cortex. *Cereb. Cortex* **21**, 1674-1694.
Rohatgi, R. and Snell, W. J. (2010). The ciliary membrane. *Curr. Opin. Cell Biol.* **22**, 541-546.
Röper, K., Corbeil, D. and Huttner, W. B. (2000). Retention of prominin in microvilli reveals distinct cholesterol-based lipid microdomains in the apical plasma membrane. *Nat. Cell Biol.* **2**, 582-592.
Rosenbaum, J. L. and Witman, G. B. (2002). Intraflagellar transport. *Nat. Rev. Mol. Cell. Biol.* **3**, 813-825.
Rukstalis, J. M. and Habener, J. F. (2007). Snail2, a mediator of epithelial-mesenchymal transitions, expressed in progenitor cells of the developing endocrine pancreas. *Gene Expr. Patterns* **7**, 471-479.
Santos, N. and Reiter, J. F. (2008). Building it up and taking it down: the regulation of vertebrate ciliogenesis. *Dev. Dyn.* **237**, 1972-1981.
Satir, P. and Christensen, S. T. (2007). Overview of structure and function of mammalian cilia. *Annu. Rev. Physiol.* **69**, 377-400.
Seeley, E. S. and Nachury, M. V. (2010). The perennial organelle: assembly and disassembly of the primary cilium. *J. Cell Sci.* **123**, 511-518.
Sfakianos, J., Togawa, A., Maday, S., Hull, M., Pypaert, M., Cantley, L., Toomre, D. and Mellman, I. (2007). Par3 functions in the biogenesis of the primary cilium in polarized epithelial cells. *J. Cell Biol.* **179**, 1133-1140.
Sloboda, R. D. (2009). Posttranslational protein modifications in cilia and flagella. *Methods Cell Biol.* **94**, 347-363.
Sorokin, S. (1962). Centrioles and the formation of rudimentary cilia by fibroblasts and smooth muscle cells. *J. Cell Biol.* **15**, 363-377.
Sorokin, S. P. (1968). Reconstructions of centriole formation and ciliogenesis in mammalian lungs. *J. Cell Sci.* **3**, 207-230.
Sotelo, J. R. and Trujillo-Cenoz, O. (1958). Electron microscope study on the development of ciliary components of the neural epithelium of the chick embryo. *Z. Zellforsch. Mikrosk. Anat.* **49**, 1-12.
Taverna, E. and Huttner, W. B. (2010). Neural progenitor nuclei IN Motion. *Neuron* **67**, 906-914.
Wang, X., Tsai, J. W., Imai, J. H., Lian, W. N., Vallee, R. B. and Shi, S. H. (2009). Asymmetric centrosome inheritance maintains neural progenitors in the neocortex. *Nature* **461**, 947-955.
Weigmann, A., Corbeil, D., Hellwig, A. and Huttner, W. B. (1997). Prominin, a novel microvilli-specific polytopic membrane protein of the apical surface of epithelial cells, is targeted to plasmalemmal protrusions of non-epithelial cells. *Proc. Natl. Acad. Sci. USA* **94**, 12425-12430.
Weisz, O. A. and Rodriguez-Boulan, E. (2009). Apical trafficking in epithelial cells: signals, clusters and motors. *J. Cell Sci.* **122**, 4253-4266.
Wodarz, A. and Huttner, W. B. (2003). Asymmetric cell division during neurogenesis in *Drosophila* and vertebrates. *Mech. Dev.* **120**, 1297-1309.